American Mineralogist, Volume 84, pages 1433–1438, 1999

Solid-state ^{29}Si MAS NMR studies of illite and illite-smectite from shale

SØREN K. LAUSEN,[1,†] HOLGER LINDGREEN,[2] HANS J. JAKOBSEN,[1] AND NIELS C. NIELSEN[1,*,†]

[1]Instrument Centre for Solid-State NMR spectroscopy, Department of Chemistry, University of Aarhus, DK-8000 Aarhus C, Denmark
[2]Clay Mineralogical Laboratory, Geological Survey of Denmark and Greenland, DK-2400 Copenhagen NV, Denmark

ABSTRACT

A new method to extract quantitative information from poorly resolved ^{29}Si magic-angle spinning (MAS) nuclear magnetic resonance (NMR) spectra of natural mixed-layer illite-smectite (I-S) clays is presented. The Si-Al distribution in layered aluminosilicates are used to link the intensities of ^{29}Si resonances from all $Q^3(n\text{Al})$ sites (n = 0, 1, 2, 3) to the tetrahedral layer aluminum substitution by applying Loewenstein's aluminum avoidance principle (no Al-O-Al linkages) extended to ensure a homogeneous distribution of charge. In addition, correlations between ^{29}Si chemical shifts and the Al substitution are established for illite resonances by computer fitting of well-resolved phyllosilicate spectra. Combination of these two constraints led to a general procedure for iterative fitting of ^{29}Si MAS NMR spectra of clay minerals containing high-charge (illite-like) and low-charge (smectite-like) sites. The applicability of the new method is demonstrated for two I-S samples from Cambrian black shale in the Baltic area and two I-S samples from Upper Jurassic oil-source rock in the Central Trough of the North Sea. In combination with data from XRD and chemical analysis, the results from ^{29}Si MAS NMR enables determination of the composition for the entire I-S particles.

INTRODUCTION

High-resolution solid-state NMR spectroscopy has become a powerful tool in studies of the composition and structure of natural and synthetic aluminosilicates (Kinsey 1985; Engelhardt and Michel 1987). In particular, ^{29}Si and ^{27}Al magic-angle-spinning NMR have provided important information on the Si and Al distribution (i.e., Si/Al ratios and ordering) in tetrahedral and octahedral sites, on sequences of charged sheets, and on structural distortions and compositional variations for a variety of phyllosilicates (e.g., vermiculite, montmorillonite, and margarite) and mixed-layer illite-smectite (I-S) minerals (e.g., rectorite). (Barron et al. 1985a, 1985b; Herrero et al. 1985, 1989; Weiss et al. 1987; Altaner et al. 1988; Jakobsen et al. 1995). In contrast, much less attention has been devoted to ^{29}Si MAS NMR studies of shale I-S that exhibits poorly resolved ^{29}Si NMR spectra with broad resonances (7–10 ppm at half height) as compared to for example those of rectorites (2–3 ppm).

In the present work, we demonstrate how simple rules for the Si-Al ordering combined with correlations between Al substitutions and ^{29}Si chemical shifts make it possible to extract detailed information on the structure and composition of illite and smectite layers in I-S from shale. These rules are established using Loewenstein's aluminum avoidance principle (Loewenstein et al. 1954) along with a homogeneous distribution of charge (Herrero et al. 1985, 1989) to determine the ^{29}Si intensity distributions and using spectra from standard minerals to obtain correlations between the ^{29}Si chemical shift and the tetrahedral Al substitution. Based on ^{29}Si NMR spectra of I-S from Cambrian black shale and shale from North Sea Upper Jurassic oil source rocks, we demonstrate that important information about the diagenetic transformation of smectite to illite layers may be obtained using the new approach for spectral analysis.

SAMPLES AND SAMPLE PREPARATION

Five natural phyllosilicate samples were used: a Na- and Ca-rich rectorite from Beatrix Mine, South Africa (sample 1); a Na-rich rectorite from Garland County, Arkansas, U.S.A. (sample 2); a $2M_2$ illite II60 from Russia (sample 3); an I-S WT5B from Tioga, New York, U.S.A. (sample 4); and a smectite SAZ from Arizona, U.S.A. (sample 5, available through the Clay Minerals Society). The I-S in sample 1 consists of paragonite, margarite, and smectite layers, while the I-S in sample 2 consists of smectite and paragonite layers as well as an impurity of 10 wt% (15 mol%) dickite (Jakobsen et al. 1995). Furthermore, we analyzed the Cambrian black Alum shale samples SL from Slagelse, Denmark (sample 6) and ES from Estonia (sample 7) as well as the Upper Jurassic shale (Kimmeridgian-Volgian age) samples 87 and 89 from the Central Through of the North Sea (samples 8 and 9, respectively). The shade samples were pre-treated with sodium hypochlorite at pH 9.0 and 100 °C for removal of organic matter and with sodium dithionite, sodium bicarbonate, and sodium citrate to remove aluminum and iron oxides and oxyhydroxides. Finally, the samples were centrifuged and the I-S fraction was isolated using the ethanol-water procedure described by Buzagh and Szepesi (1955).

*E-mail: ncn@kemi.aau.dk
† Present address: Laboratory for Biomolecular NMR Spectroscopy, Department of Molecular and Structural Biology, Science Park, University of Aarhus, DK-8000 Aarhus C, Denmark.

0003-004X/99/0009–1433$05.00

NMR SPECTROSCOPY

The ^{29}Si MAS NMR spectra were recorded on a Varian XL-300 NMR spectrometer (7.1 T, 59.59 MHz for ^{29}Si) using a home-built MAS probe with 7 mm PSZ (partially stabilized zirconia) rotors. The spectra were obtained using single-pulse RF excitation employing a pulse width of 5 μs for a field strength of 50 kHz, 5–60 s recycle delay to ensure quantitatively reliable spectra, and MAS with a spinning speed in the range 5–7 kHz. ^{29}Si isotropic chemical shifts are relative to external TMS. Numerical calculations and iterative fitting of experimental ^{29}Si MAS NMR spectra were carried out using a home-made FORTRAN-77 simulation program combined with the MINUIT optimization package (James and Roos 1977). This allows appropriate combinations of Monte Carlo, Simplex, and steepest-descend multivariate optimization. All calculations were performed on a Sun ULTRA-SPARC-1 workstation.

RESULTS AND DISCUSSION

Si-$^{[4]}$Al distribution

As discussed in detail (Vega 1983; Engelhardt and Michel 1987; Baron et al. 1985b; Herrero et al. 1985), the distribution of Si and Al in the tetrahedral sheets of silicates, and thereby the relative intensities of the four ^{29}Si(nAl) resonances from the different Q^3(nAl) sites, obey the restrictions imposed by Loewenstein's rule (LR) (Loewenstein et al. 1954). Furthermore, there is evidence that the Al cations are homogeneously distributed as described by Herrero et al. (1985, 1989) in terms of their so-called Homogeneous Distribution of Charges (HDC) model. Combination of these two models forms an essential element in our method used for the analysis of complex, poorly resolved ^{29}Si MAS NMR spectra. The reason is that the intensities of the four ^{29}Si (nAl) resonances become dependent on a single variable, i.e., the degree of $^{[4]}$Al substitution x = $^{[4]}$Al/($^{[4]}$Al + Si) in the tetrahedral sheet, rather than four independent variables.

By combining the simulation procedures proposed by Barron et al. (1985b) and Herrero et al. (1985), it is a straightforward matter to relate the signal intensities according to LR and HDC models as demonstrated in Figure 1. The simulations are based on a square matrix with 1300 tetrahedral sites in hexagonal patterns, which for a given x are filled with Si and Al in a random manner. Subsequently, the Si and Al positions are interchanged to reduce the number of Al-O-Al linkages. For LR this procedure is continued until all Al-O-Al bridges are removed. For HDC the ordering is further improved to ensure a homogeneous distribution of the local charge (i.e., $^{[4]}$Al). For example, the number of hexagons with 0 or 3 Al is minimized when x is between 1/6 and 1/3. For both models the simulation leads to four signal intensities I[Si(nAl)] for any value of x. For LR the signal intensities relate favorably to the well-known binominal formulas $(1\text{-}p)^3$, $3p(1\text{-}p)^2$, $3p^2(1\text{-}p)$ and p^3 [p = $^{[4]}$Al/Si = $x/(1\text{-}x)$] for I[Si(nAl)] with n = 0, 1, 2, and 3, respectively, as indicated by the solid lines in Figure 1a (Engelhardt et al. 1987; Herrero et al. 1989). Minor discrepancies between the binominal distribution and the simulated intensities for $x \geq 0.35$ may be attributed to difficulties in distributing Al randomly in the hexagonal pattern when the concentration of Al is large.

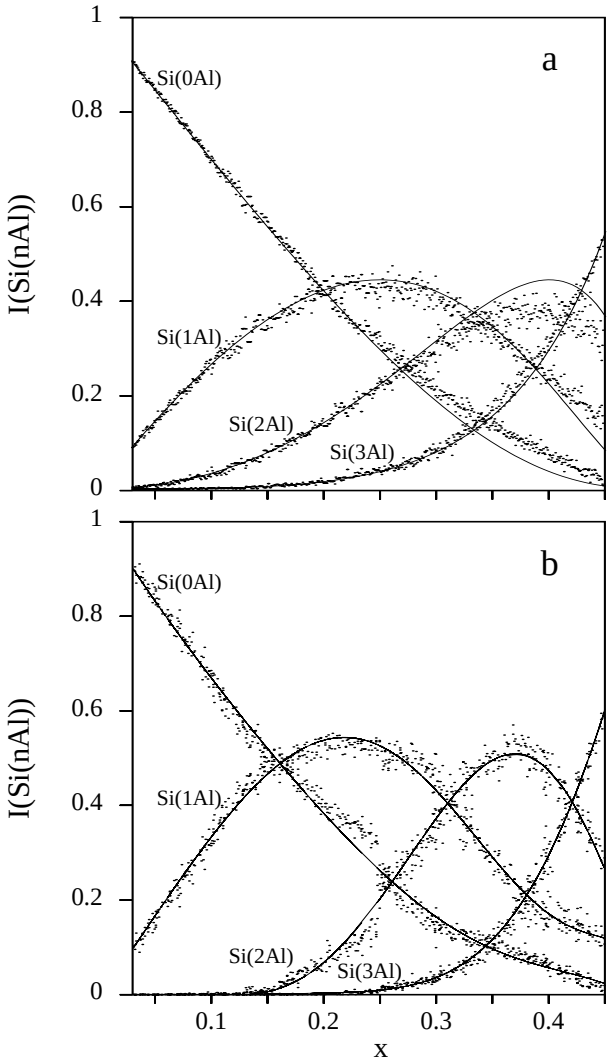

FIGURE 1. Relative signal intensities calculated for the four Si(nAl), n = 0, 1, 2, and 3, signal components in ^{29}Si MAS NMR spectra of aluminosilicates with different tetrahedral aluminum content, x = $^{[4]}$Al / ($^{[4]}$Al + Si). The dots correspond to simulated distributions of Si and Al according to (**a**) Loewenstein's rule and (**b**) homogeneous distribution of charges. The solid lines in (**a**) result from the well-known binominal distributions (Engelhardt et al. 1987; Herrero et al. 1989), while those in (**b**) result from fitting of the signal intensities using ninth order polynomials with the coefficients listed in Table 1 (see text).

For HDC the intensities may be fitted to a high-order polynomium in order to obtain numerical expressions for the signal intensities as function of x. The resulting intensity curves are given in Figure 1b and the corresponding coefficients in Table 1. We note that the HDC intensity curves presented by Herrero et al. (1989) differ marginally from those in Figure 1b, most likely because of slightly different criteria when defining details in the local balance of charge. It is also noted that the difference between LR and HDC mainly lies in the increased I[Si(1Al)] for HDC at low Al contents. In the following our spectral analysis is based on the HDC model.

TABLE 1. Coefficients a_i for the homogeneous distribution of charge (HDC) model

	i									
n	0	1	2	3	4	5	6	7	8	9
0	1.01	–3.78	4.02	–2.4	–22.7	53.5	71.6	443.1	–2186.7	1969.5
1	–0.01	3.47	1.81	–17.5	–49.4	–49.2	89.4	645.5	1587.4	–4086.6
2	–0.04	2.12	–25.4	77.9	168.4	–578.0	21.9	–659.7	2215.9	–353.5
3	0.01	–0.33	3.57	–13.2	17.6	–35.3	73.1	256.4	380.0	–1387.9

Note: a_i is for the ninth–order polynomials $I[\mathrm{Si}(n\mathrm{Al})] = \sum_{i=0}^{9} a_i x^i$ relating the intensity for the four Si(*n*Al) resonances, n = 0, 1, 2, 3, to the tetrahedral layer aluminum substitution x.

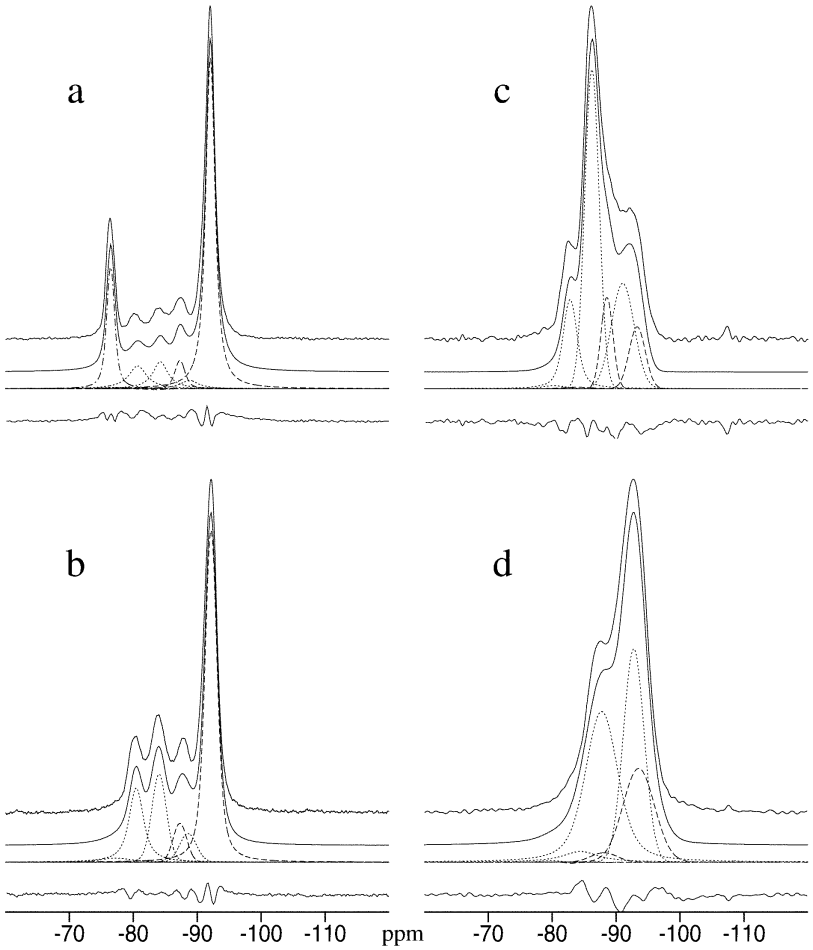

FIGURE 2. ^{29}Si MAS NMR spectra of the four standard illite and I-S samples (**a**) 1, (**b**) 2, (**c**) 3, and (**d**) 4. The upper traces represent experimental spectra, the second uppermost traces the results of our new approach to iterative spectral analysis in terms of the individual resonances given below the calculated spectrum, and the bottom trace the difference between the experimental and calculated spectra. Illite is represented by dotted curve, smectite and dickite by dashed curve, and margarite by dash-and-dot curve. The calculated spectra correspond to the parameters given in Table 2.

^{29}Si chemical shift vs. Si/$^{[4]}$Al ratio

According to Kinsey et al. (1985) and Weiss et al. (1987) the isotropic ^{29}Si chemical shifts (δ_{iso}) for layer silicates with identical octahedral sheets display strong correlations with structural distortions induced by variation in the Al content for the tetrahedral sheets. Provided accurate correlations can be established empirically, this feature may greatly facilitate simulation and iterative fitting of ^{29}Si MAS NMR spectra for natural clay minerals. In this manner, the chemical shifts describing the various Si(*n*Al) substitution patterns may be related to the value of x for the sheet alone instead of independent variables for the various resonances. This simple correlation assumes that minor dependences of δ_{iso} on interlayer cations, tetrahedral cation-oxygen bond lengths, and cation substitution in the octahedral sheet can be neglected (Weiss et al. 1987).

To establish δ_{iso} vs. x correlations for relevant Si(*n*Al) substitutions we have analyzed ^{29}Si MAS NMR spectra for a series of typical illite and I-S samples. Our analysis involves one pure illite sample, one I-S, and two rectorites exhibiting similar structural parameters but different Al substitution. Samples with a relatively high illite Al substitution ($x_I \approx 0.2$–0.35) and narrow ^{29}Si resonances (2–3 ppm) were selected to ensure well-resolved Si(*n*Al) resonances for n = 0, 1, and 2. By simulation of the experimental ^{29}Si MAS NMR spectra for these samples (Fig. 2) using iterative fitting with free variation of line positions, shapes, and intensities, linear correlations between δ_{iso}

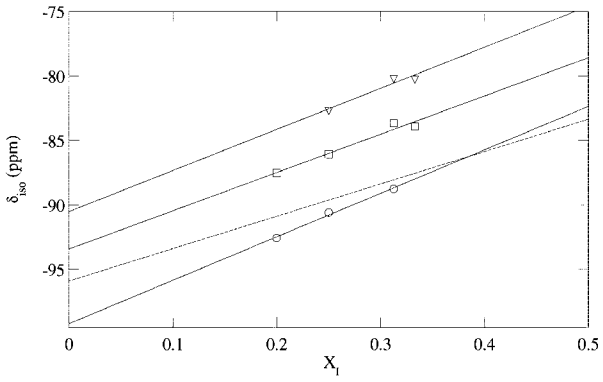

FIGURE 3. Correlation between illite ^{29}Si isotropic chemical shifts (δ_{iso}) and the tetrahedral aluminum content x_I determined from the experimental spectra in Figure 2. The correlations correspond to Si(0Al) (circle), Si(1Al) (square), Si(2Al) (triangle), while the dashed line corresponds to a previous Si(0Al) correlation from Weiss et al. (1987). The following correlations are obtained by linear regression (correlation coefficient for linear regression in parenthesis): δ_{iso}[Si(0Al)] = 33.7 x_I – 99.2 ppm (R^2 = 0.992), δ_{iso}[Si(1Al)] = 29.7 x_I – 93.4 ppm (R^2 = 0.962), and δ_{iso}[Si(2Al)] = 31.8 x_I – 90.5 ppm (R^2 = 0.935).

and x_I for the three relevant Si(nAl) resonances have been established as shown in Figure 3. For comparison, Figure 3 also includes the Si(0Al) correlation earlier presented by Weiss et al. (1987). The slight difference between the two Si(0Al) correlation curves could be ascribed to differences in the octahedral sheets. The available model samples did not allow similar correlations for the Si(3Al) resonance to be derived.

Our modeling is based on tetrahedral sheets of low-charge smectite (having x_S values between 0.0 and 0.05) and illite. Two-phase I-S models have formed the basis for the vast majority of studies of clay minerals described so far. However, Drits et al. (1997) based on XRD studies of the I-S samples 87 and 89 recently suggested an alternative model with additional contributions from high-charge smectite and vermiculite interlayers. I-S may even be composed of tetrahedral sheets having a continuous degree of substitution in the range x_S = 0.0–0.18. This structure can result from solid-state substitution of Al for Si until dehydration and fixation of interlayer cations takes place and illite interlayers are formed, the solid-state interlayer transformation (Drits et al. 1997).

Numerical simulations and iterative fitting

Considering I-S, ^{29}Si MAS NMR spectra may contain up to eight resonances each associated with a frequency, line width, line-shape function, and intensity. These parameters along with the I/S ratio lead to 33 variables relevant for analysis through iterative fitting. The number of free variables may be reduced to 20 by considering only Si(0Al) and Si(1Al) resonances with fixed line positions for smectite (–93.5 and –88.1 ppm, respectively) and using fixed resonance frequency (–79.6 ppm), line width, and line-shape function for the low-intensity Si(3Al) illite resonance ($x_I \approx 0.2$). Furthermore, by coupling of the illite and smectite resonance intensities to x_I and x_S using the HDC model and the illite resonance frequencies to x_I through the δ_{iso} vs. x_I correlation the number of variables is reduced to 13. Among these are the structurally important I/S ratio, x_I, and x_S along with 10 variables describing the width and shape (specified to a mixed Lorentzian/Gaussian line shape) for the five dominant resonances.

The line widths and Lorentzian/Gaussian fractions, reflecting the chemical shift dispersions and the transverse relaxation, depend on the structure of the second coordination sphere and the presence of paramagnetic impurities (Engelhardt and Michel 1987). Reasonable estimates (initial values) and limiting values have been obtained empirically by iterative fitting of ^{29}Si MAS NMR spectra for a variety of clay minerals and model samples. For example, the SAZ smectite (sample 5) reveals a Si(0Al) resonance with a line width of 230 Hz, which imposes a starting value and a realistic upper limit of about 300 Hz for the line width. To allow variations in the local order and cation composition of the samples and to avoid local minima in the root-mean-square (RMS) deviation between experimental and simulated spectra, the iterative fitting initially restricts variation of the I/S ratio, x_I, and x_S to the typical ranges of 0.8–1.0, 0.17–0.25, and 0.03–0.1, respectively. Subsequently, all 13 parameters are set free within less restrictive limits in the iterative fitting.

I-S structures

As a first demonstration of the applicability of the procedure for spectral simulation and iterative fitting described above, we have analyzed the ^{29}Si MAS NMR spectra of the standard I-S and illite samples (samples 1-4) as shown in Figure 2. The optimum simulated spectra and the contributing resonances are shown below the experimental spectra. The two rectorites (samples 1 and 2, Figs. 2a and 2b) represent typical 2:1 phyllosilicates for which high-resolution ^{29}Si MAS spectra may be obtained and standard spectral analysis allows determination of parameters for comparison with those resulting from our new approach. The II60 illite (Fig. 2c) and the WT5B I-S (Fig. 2d) samples, provide examples of ^{29}Si MAS NMR spectra exhibiting less favorable resolution. For all samples iterative fitting results in calculated spectra which compare well with the experimental spectra (see difference plots). For the rectorites we obtain parameters for the composition of the illite, paragonite, smectite, and margarite layers (Table 2) which are essentially equal to those reported previously (Jakobsen et al. 1995). Considering the II60 illite and the WT5B I-S samples the calculated spectra indicate a significantly larger amount of smectite than the small amounts expected to be present in an illite and to the amounts found by XRD. We attribute the additional amounts of smectite measured by NMR to smectite substitution patterns in the top and bottom tetrahedral sheets of the coherent scattering domains (Altaner et al. 1988; Jakobsen et al. 1995). For the $2M_2$ illite II60 (sample 3) and the WT5B I-S (sample 4) the calculated spectra correspond to Si/$^{[4]}$Al ratios of 3.1 (x_I = 0.24) and 4.2 (x_I = 0.19), respectively, for the illite tetrahedral sheets. The Si/$^{[4]}$Al ratios of 3.4 and 5.6 determined by NMR for the whole samples of II60 and WT5B, respectively, are in good agreement with the values of 3.0 and 5.0 determined by total chemical analysis (V.A. Drits, personal communication).

The performance of our new approach for the analysis of low-resolution ^{29}Si MAS NMR spectra is demonstrated in Figure 4 by iterative fitting of the spectra for Cambrian and Jurassic I-S. Clearly, these spectra would be extremely difficult to analyze using standard spectral curve fitting procedures to obtain information about structure and composition. Employing iterative spectral analysis based on the HDC model and the δ_{iso} vs. x correlations, it is possible to resolve the spectra in terms of resonances from illite and smectite as demonstrated in Figure 4. The corresponding parameters are given in Table 2.

For all samples, the Si/$^{[4]}$Al ratio in the illite layers is determined to be close to 4.0 with a variation of 0.4 corresponding to a variation of ±2% in the Al substitution. This conforms well with calculations based on chemical analysis as do the significantly lower Al substitution in the smectite layers. Of greater interest is the proportion of illite layers being influenced by

TABLE 2. Composition of rectorite, illite, smectite, and I-S from Cambrium black shale and North Sea Upper Jurassic oil-source rock shale (see text)

Sample	$Illite_{NMR}$* (%)	$Illite_{XRD}$† (%)	$Paragonite_{NMR}$* (%)	Margarite $_{NMR}$* (%)	$Smectite_{NMR}$* (%)	Dickite (%)	x_I (Si/$^{[4]}$Al)‡	x_S (Si/$^{[4]}$Al)‡	N§	Illite Top and bottom
1. Beatrix rectorite			20	17	63		0.31 (2.23)	0.02 (40)	10	‖
2. Arkansas rectorite			39		46	15#	0.32 (2.16)	0.03 (32)	8	
3. II60	80				20		0.24 (3.12)	0.17 (4.9)		
4. WT5B	77	87			23		0.19 (4.22)	0.02 (40)		
5. SAZ					100			0.03 (30)		
6. ES	81	88			19		0.18 (4.44)	0.03 (33)	6.8	0.40
7. SL	89	96			11		0.20 (3.91)	0.04 (24)	7.7	0.42
8. 87	80	80			20		0.20 (4.03)	0.02 (40)	5.1	0.80
9. 89	85	84			16		0.21 (3.66)	0.08 (11)	5.3	0.89

Note: 95% confidence intervals for the structural parameters of samples 6–9 are estimated by investigating the RMS values around the global minima resulting in the following precisions; illite content ± 0.04, x_I ± 0.005, and x_S ± 0.05.
* Proportion of tetrahedral sheets determined by NMR.
† Proportion of interlayers determined by XRD.
‡ x = $^{[4]}$Al /($^{[4]}$Al +Si) calculated using $Si/^{[4]}Al = 3\sum_{n=0}^{2} I[Si(nAl)] / \sum_{n=0}^{2} n I[Si(nAl)]$.
§ Average number of 2:1 layers in the coherent scattering domains determined by XRD.
‖ 6% margarite + 4% paragonite (Jakobsen et al. 1995).
Jakobsen et al. 1995.

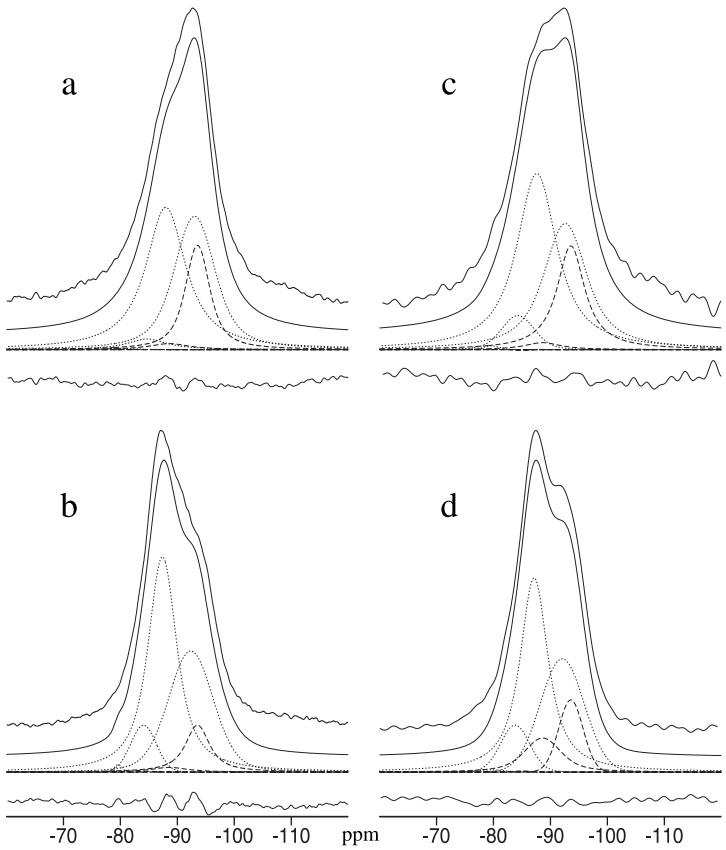

FIGURE 4. ^{29}Si MAS NMR spectra of natural shale clay minerals from (**a**) Estonia (sample 6) and (**b**) Slagelse, Denmark (sample 7) as well as mixed I-S layer clay minerals from Upper Jurassic oil-source rock (**c**) 87 (sample 8) and (**d**) 89 (sample 9) obtained from the Central Trough of the North Sea. The traces below the experimental spectra (upper trace) contain optimum calculated spectra, their components, and the difference between experimental and calculated spectra. The calculated spectra were obtained using the novel approach for spectral analysis described in this work and correspond to the parameters given in Table 2. Symbols are as in Figure 2.

diagenesis in the claystones. The smectite to illite transformation provides information about sedimentation and oil generation. It is therefore of interest to determine the illite content with high precision. ^{29}Si MAS NMR provides compositional information independently of long-range order and is thereby capable of measuring the illite content for the entire I-S particle as demonstrated recently (Jakobsen et al. 1995). Furthermore, by using the complementary information from XRD [total number of 2:1 layers and the fraction of illite interlayers in the coherent scattering domains (CSD)] and solid-state NMR (total amount of illite tetrahedral sheets), it is possible to determine the composition and layer structure (sequences of charged sheets) for the entire CSD.

For the two Baltic shale clay samples from Estonia (sample 6) and Slagelse, Denmark (sample 7) iterative fitting of the ^{29}Si MAS NMR spectra leads to proportions of illite tetrahedral sheets of 0.81 ± 0.04 and 0.89 ± 0.04, respectively. These numbers may be compared with the proportion of illite interlayers of 0.88 ± 0.01 and 0.96 ± 0.01 determined by XRD which, along with the average of 6.2 and 7.0 for the number of 2:1 layers in the CSD, indicates that the top and bottom tetrahedral sheets have significantly lower proportions of illite compared to the average for the CSD. Specifically, only 0.40 and 0.42 of the top and bottom tetrahedral sheets are illitic for the Cambrian I-S from Estonia and Slagelse, respectively.The illite content in both interlayers and top and bottom tetrahedral sheets is somewhat larger for the Slagelse sample than for the Estonia samples. This is understandable and expected from a geological point of view because the I-S from Slagelse, in contrast to the one from Estonia, has been subject to incipient metamorphism causing smectite to illite transformation. A similar analysis of the ^{29}Si MAS NMR spectra for the two Upper Jurassic North Sea I-S oil-source rock clays, 87 and 89, reveals contents of illite tetrahedral sheets of 0.80 ± 0.04 and 0.85 ± 0.04, respectively. Compared to the fraction of illite interlayers of 0.80 ± 0.01 and 0.84 ± 0.01 determined by XRD, these numbers indicate that interlayers and top and bottom tetrahedral sheets have approximately the same proportion of illite and smectite.

The results in this work demonstrate that it is possible to extract detailed structural information from ^{29}Si MAS NMR spectra of natural clay minerals exhibiting poor spectral resolution. It is anticipated that the new method will find important applications for studies of synthetic and natural layer silicates to obtain information about layer charges and sequences of charged sheets as well as about physical properties such as swelling, cation-exchange capacity, and catalytic capability.

ACKNOWLEDGMENTS

The use of the facilities at the Instrument Centre for Solid-State NMR Spectroscopy, University of Aarhus, is acknowledged. This research has been supported by equipment grants from the Danish Natural Science Research Council, the Danish Technical Research Council, Direktør Ib Henriksens Fond, Carlsbergfondet, and Aarhus University Research Foundation. This paper is published with the permission of the Geological Survey of Denmark and Greenland. We thank V.A. Drits, A.L. Salyn, and B.A. Sakharov for constructive discussions and V.A. Drits for providing sample II60.

REFERENCES CITED

Altaner, S.P., Weiss Jr., C.A., and Kirkpatrick, R.J. (1988) Evidence from ^{29}Si NMR for structure of mixed-layer illite/smectite clay minerals. Nature, 331, 699–702.

Barron, P.F., Slade, P., and Frost, R.L. (1985a) Solid-State Silicon-29 Spin-Lattice Relaxation in Several 2:1 Phyllosilicate Minerals. Journal of Physical Chemistry, 89, 3305–3310.

———(1985b) Ordering of aluminum in tetrahedral sites in mixed-layer 2:1 phyllosilicates by solid-state high-resolution NMR. Journal of Physical Chemistry, 89, 3880–3885.

Buzagh, A. and Szepesi, K. (1955) A colloid-chemical method for the determination of the montmorillonite content in bentonites. Acta Chimica Hungarica, 5, 287–298.

Drits, V.A., Sakharov, B.A., Lindgreen, H., and Salyn, A. (1997) Sequential structural transformation of illite-smectite-vermiculite during diagenesis of Upper Jurassic shales from the North Sea and Denmark. Clay Minerals, 32, 351–371.

Engelhardt, G. and Michel, D. (1987) High resolution solid state NMR of silicates and zeolites, Wiley, Chichester, U.K.

Herrero, C.P., Sanz, J., and Serratosa, J.M. (1985) Tetrahedral cation ordering in layer silicates by ^{29}Si NMR spectroscopy. Solid State Communications, 53, 151–154.

———(1989) Dispersion of charge deficits in the tetrahedral sheet of phyllosilicates. Analysis from ^{29}Si NMR spectra. Journal of Physical Chemistry, 93, 4311–4315.

Jakobsen, H.J., Nielsen, N.C., and Lindgreen, H. (1995) Sequences of charged sheets in rectorite. American Mineralogist, 80, 247–252.

James, F. and Roos, M. (1975) MINUIT—A System for Function Minimization and Analysis of the Parameter Errors and Correlations. Computer Physics Communications, 10, 343–367.

Kinsey, R.A., Kirkpatrick, R.J., Hower, J., Smith, K.A., and Oldfield, E. (1985) High resolution aluminum-27 and silicon-29 nuclear magnetic resonance spectroscopic study of layer silicates, including clay minerals. American Mineralogist, 70, 537–548.

Loewenstein, W. and Loewenstein, M. (1954) The distribution of aluminum in the tetrahedra of silicates and aluminates. American Mineralogist, 39, 92–97.

Vega, A.J. (1983) A statistical approach to the interpretation of silicon-29 NMR of zeolites. In G.D. Stucky and F.G. Dwyer, Eds., Intrazeolite chemistry, p. 217–230. American Chemical Society Symposium Series, 218.

Weiss Jr., C.A., Altaner, S.P., and Kirkpatrick, R.J. (1987) High-resolution ^{29}Si NMR spectroscopy of 2:1 layer silicates: Correlations among chemical shift, structural distortions, and chemical variations. American Mineralogist, 72, 935–942.

MANUSCRIPT RECEIVED NOVEMBER 3, 1998
MANUSCRIPT ACCEPTED MARCH 25, 1999
PAPER HANDLED BY JONATHAN F. STEBBINS